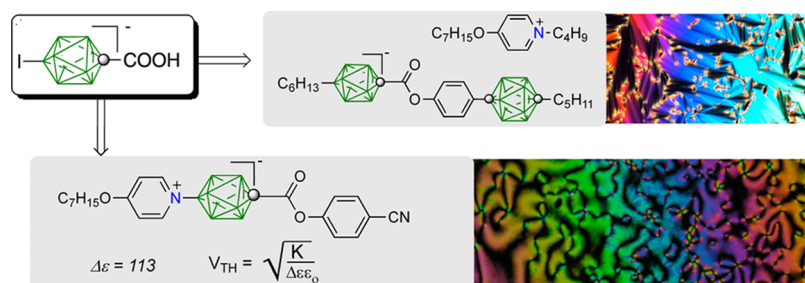# Functionalization of the [*closo*-1-CB$_9$H$_{10}$]$^−$ Anion for the Construction of New Classes of Liquid Crystals

BRYAN RINGSTRAND[†] AND PIOTR KASZYNSKI[*, †, ‡]

[†]*Organic Materials Research Group, Department of Chemistry, Vanderbilt University, Nashville, Tennessee 37235, United States, and* [‡]*Faculty of Chemistry, University of Łódź, Tamka 12, 91403 Łódź, Poland*

CONSPECTUS

The [*closo*-1-CB$_9$H$_{10}$]$^−$ anion is a member of an extensive family of σ-aromatic *closo*-boranes that possess impressive stability and functionalization characteristics. In contrast to its bigger, more extensively studied brother, the [*closo*-1-CB$_{11}$H$_{12}$]$^−$ anion, convenient access to the [*closo*-1-CB$_9$H$_{10}$]$^−$ anion has only been recently established, and researchers have only begun to develop and understand its fundamental chemistry.

The geometrical and electronic properties of the [*closo*-1-CB$_9$H$_{10}$]$^−$ anion make it an attractive structural element of novel classes of either zwitterionic or ionic liquid crystals suitable for electro-optical and ion transport applications, respectively. Such materials require a 1,10-difunctionalized [*closo*-1-CB$_9$H$_{10}$]$^−$ anion that permits for the formation of molecules of elongated shape. The covalent attachment of an onium fragment or the use of a counterion compensates for the negative charge. This Account highlights the progress made in the advancement and understanding of the fundamental chemistry of the [*closo*-1-CB$_9$H$_{10}$]$^−$ anion. We also describe the development of 1,10-difunctionalized derivatives as key intermediates in the preparation of new classes of liquid crystalline materials.

We obtained the first isomerically pure 1,10-difunctionalized derivative of the [*closo*-1-CB$_9$H$_{10}$]$^−$ anion, iodo acid [*closo*-1-CB$_9$H$_8$-1-COOH-10-I]$^−$, from decaborane through the Brellochs reaction. Functional group transformation of the C(1)-carboxyl group led to a 1-amino derivative and, subsequently, to a synthetically valuable 1-dinitrogen derivative. The latter exhibits reactivity typical for PhN$_2^+$ and undergoes diazocoupling and Gomberg−Bachmann arylation reactions. The B(10)-iodine participated in Negishi alkylation and Buchwald−Hartwig amination reactions, leading to 10-hexyl and 10-amino carboxylic acids, respectively. We converted the 10-amino carboxylic acid to a 10-dinitrogen acid [*closo*-1-CB$_9$H$_8$-1-COOH-10-N$_2$], which proved to be synthetically valuable in the preparation of 10-pyridinium and 10-sulfonium zwitterionic acids and their liquid crystalline esters. We investigated several intermediates using structural, spectroscopic, and kinetic methods.

Introduction

The discovery of polyhedral boron clusters was one of the most exciting developments in inorganic chemistry of the last century. These boron clusters are characterized by three-center two-electron bonds, which were described by William Lipscomb. Lipscomb's discovery, for which he was awarded the Nobel Prize in 1976, revolutionized the way chemists understood chemical bonding.[1] As a result of this unique bonding characteristic, certain boron clusters exhibit σ-aromaticity and are exceptionally stable chemically, electrochemically, and thermally.[2] These properties opened up possibilities for the application of boron clusters in a variety of fields, such as treatment of nuclear waste and cancer, catalysis, and materials science.[3]

The carboranes and the *closo*-borates have dominated the literature due to their availability and relative ease of functionalization.[4] On the other hand, *closo*-monocarbaborates, including the [*closo*-1-CB$_9$H$_{10}$]$^-$ (**1**) and [*closo*-1-CB$_{11}$H$_{12}$]$^-$ (**2**) anions (Figure 1), have garnered less attention.

The negative charge in anions **1** and **2** is delocalized, making the clusters non-nucleophilic and weakly coordinating anions.[5] Critical for exploiting the properties of **1** and **2** is the established chemistry of both the carboranes and borates. Deprotonation of the C−H vertex affords a carboranyl anion capable of reacting with electrophiles.[4] Conversely, the B−H vertices are subject to electrophilic substitution, leading to, for example, B-iodo derivatives, that have been used in Pd-catalyzed coupling reactions.[4]

Of the *closo*-monocarbaborates **1** and **2**, the [*closo*-1-CB$_{11}$H$_{12}$]$^-$ anion (**2**) has been thoroughly investigated, and as a result, its chemistry is more developed.[6] On the other hand, the [*closo*-1-CB$_9$H$_{10}$]$^-$ anion (**1**) has been mostly unexplored due to poor accessibility. Anion **1** was discovered in 1971 by W. H. Knoth as a product of thermal comproportionation of the [*nido*-7-CB$_{10}$H$_{13}$]$^-$ anion.[7] Other methods expanded on Knoth's work,[8] but the preparation of 1,10-difunctionalized species of anion **1** remained elusive. C-substituted derivatives were rare before 2000,[9,10] and electrophilic monohalogenation was shown to occur solely at the 6-position.[11]

This situation changed with development of the Brellochs reaction, which permitted for the synthesis of a variety of C(1) substituted derivatives of **1** and opened up new possibilities for studying the {*closo*-1-CB$_9$} framework.[12,13] According to Brellochs, the reaction of decaborane, B$_{10}$H$_{14}$, with aldehydes in alkaline solution produces either [*arachno*-6-CB$_9$H$_{13}$-6-R]$^-$ (**I**) or [*nido*-6-CB$_9$H$_{11}$-6-R]$^-$ (**II**) derivatives
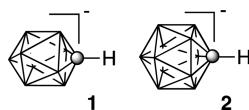
(Scheme 1).[13] These species undergo oxidative closure of the {CB$_9$} framework, giving [*closo*-2-CB$_9$H$_9$-2-R]$^-$ (**III**) derivatives, and subsequent thermal rearrangement of **III** provides the more thermodynamically stable [*closo*-1-CB$_9$H$_9$-1-R]$^-$ (**IV**) isomer. The Brellochs reaction works well with formaldehyde and electron deficient aldehydes.[12−16]

Despite an increase in the number of [*closo*-1-CB$_9$H$_{10}$]$^-$ derivatives, 1,10-difunctionalized species were still practically unknown. Since electrophilic monosubstitution of anion **1** occurs nearly exclusively at the 6-position,[11] functionalization of the 10-position posed a serious challenge. However, it was demonstrated that halogenation of [*closo*-2-CB$_9$H$_9$-2-Ph]$^-$ (**III** in Scheme 1) occurred regioselectively at the 7-position, which after thermal rearrangement gave a mixture of 1,10- and 1,6-disubstituted {*closo*-1-CB$_9$} derivatives.[12] Although [*closo*-1-CB$_9$H$_9$-1-Ph-10-I]$^-$ was isolated and its molecular structure established, a practical procedure for the preparation of this or other 1,10-disubstituted derivatives was not pursued.[12] Such isomerically pure 1,10-disubstituted derivatives could be used in the synthesis of linear molecular systems[17] and in our liquid crystals program in particular.[18]

Liquid crystals are anisotropic fluids formed by anisometric molecules typically containing both a rigid core and flexible substituents, e.g. alkyl chains. One type of such anisometric molecules is elongated, rodlike (calamitic), represented in Figure 2. Typically, the molecular core contains cyclic elements, such as benzene ring, cyclohexane, bicyclo[2.2.2]octane, or a heterocycle substituted in the antipodal positions. The rigid core elements may be connected directly or linked through functional groups such as esters, imines, and azo or ethylene spacers.[19] In such systems, liquid crystallinity appears as a balance between ordering forces
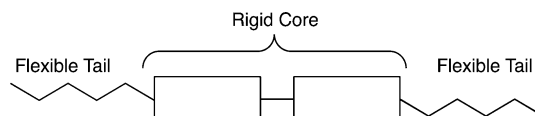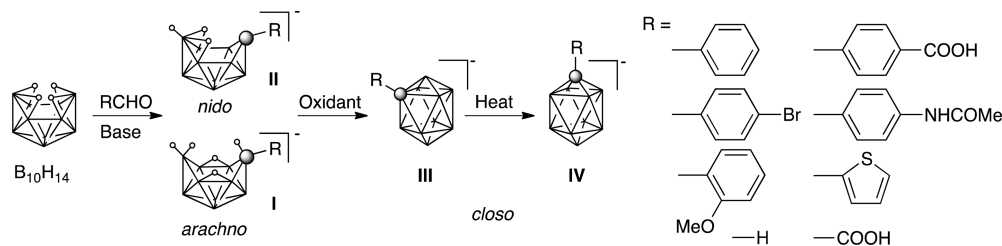

FIGURE 1. [*closo*-1-CB$_9$H$_{10}$]$^-$ anion **1** and [*closo*-1-CB$_{11}$H$_{12}$]$^-$ anion **2**. The sphere represents a carbon atom, and all other vertices are BH groups.

FIGURE 2. Schematic representation of a rodlike molecule.

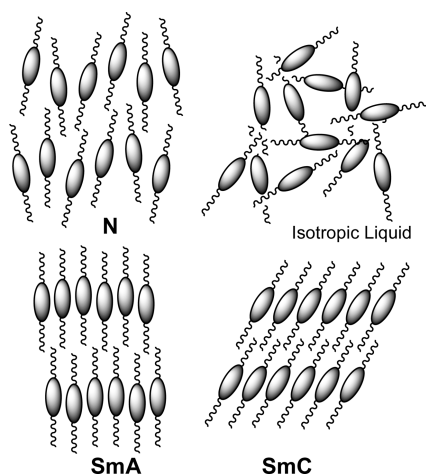**SCHEME 1.** Brellochs Reaction and Preparation of [*closo*-1-CB$_9$H$_9$-1-R]$^-$ (**IV**)

FIGURE 3. Schematics of nematic (N), smectic A (SmA), smectic C (SmC), and an isotropic liquid. The ovals represent the molecular rigid core, and the squiggly lines alkyl chains.

of the rigid cores and disordering effects of the alkyl chains.

Rodlike molecules typically form nematic and smectic liquid crystalline phases (Figure 3). The nematic phase is the least organized phase, but it is the most widely employed in the liquid crystal display (LCD) industry. Nematic liquid crystals formed by polar anisometric molecules undergo reorientation of molecules in an electric field, changing the optical properties of the material. This electrooptical (EO) effect is fundamental to virtually all LCD technologies. The threshold voltage of the EO effect is approximately inversely proportional to the magnitude of the molecular dipole. Therefore, nematic liquid crystals and nematic phase-compatible additives with large longitudinal or transverse dipole moments are sought after for formulation of nematic materials for display applications.

Ion pairs of charged anisometric molecules may also form liquid crystalline phases. Such ionic liquid crystals (ILC) typically form smectic phases and often exhibit high ionic conductivity, making them attractive electrolytes for solid-state batteries and dye-sensitized solar cells. The vast majority of ILC are comprised of an organic cation that drives mesogenicity, such as pyridinium, with a small counterion for charge compensation. However, anisometric anions with Li$^+$ counterion are desired for battery applications.

These challenges in soft materials can be addressed by using the [closo-1-CB$_9$H$_{10}$]$^-$ anion (**1**) as a structural element of liquid crystals. Thus, disubstitution of cluster **1** in positions 1 and 10 with appropriate fragments will lead to anisometric molecules, which is a prerequisite for the formation of liquid crystalline phases. Compensation of the negative charge of
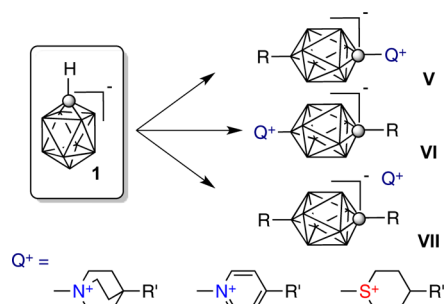

FIGURE 4. Zwitterions **V** and **VI** and ion pair **VII**. Q$^+$ represents an onium fragment such as ammonium, sulfonium, or pyridinium, or a metal cation (for **VII** only). R and R' represent organic fragments.

the anion with an onium substituent Q$^+$ leads to zwitterions **V** and **VI** having large longitudinal dipole moments. Such molecules would be of substantial interest for electro-optical applications. On the other hand, charge compensation with a counterion may lead to anion-driven ILCs capable of supporting cation transport (**VII**) (Figure 4).

Despite the potential of the [closo-1-CB$_9$H$_{10}$]$^-$ anion (**1**) as a structural element of new classes of liquid crystals, understanding of its fundamental chemistry and availability of 1,10-difunctionalized derivatives were lacking. This review will highlight the development of the fundamental chemistry of anion **1** and its application as a structural element of new liquid crystalline materials.

The First Isomerically Pure 1,10-Disubstituted {closo-1-CB$_9$} Cluster. We envisioned 1,10-disubstituted iodo acid [closo-1-CB$_9$H$_8$-1-COOH-10-I]$^-$ (**3**) as a general precursor to compounds **V**–**VII** (Figure 4). The B(10) iodine provides a means to introduce alkyl, aryl, or amino functionality *via* Pd-catalyzed coupling reactions. The C(1) carboxyl in **3** offers another convenient synthetic handle, that can be converted to esters or an amino group using classical organic synthetic methods. The amino group at either the C(1) or B(10) positions can be transformed into a quinuclidine ring or synthetically valuable dinitrogen derivatives.

The iodo acid **3** was prepared from [closo-2-CB$_9$H$_9$-2-COOH] (**4**), obtained according to the Brellochs method.[15] Iodination of **4** with *N*-iodosuccinimide (NIS) gave 7-iodo derivative **5**, which was thermolyzed, giving a mixture of iodo acids **3** and **6**. Isomerically pure iodo acid **3** was obtained by crystallization (Scheme 2).[20,21]

**Transformations of [closo-1-CB$_9$H$_8$-1-COOH-10-I]$^-$.** With iodo acid **3** available in multigram quantities and 10% overall yield from B$_{10}$H$_{14}$,[21] synthetic transformations of the carboxyl group and iodine at positions C(1) and B(10), respectively, to an amino group in the context of accessing structures **V**−**VII** were investigated. Thus, the C(1) carboxyl

SCHEME 2. Preparation of Iodo Acid **3**
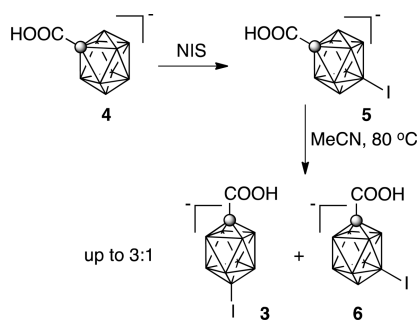
SCHEME 3. Preparation of Amine **8**
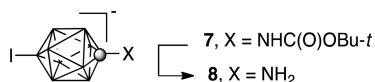
SCHEME 4. Preparation of Amino Acid **11**

up to 5:1 ratio
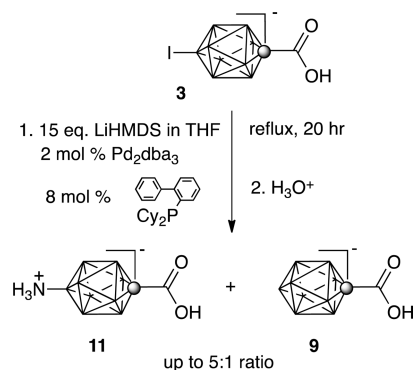
was converted into an amino group using a modified Curtius rearrangement, *via tert*-butyl carbamate **7**, providing [*closo*-1-CB$_9$H$_8$-1-NH$_2$-10-I]$^-$ (**8**, Scheme 3).[22] Initial details of this transformation were developed for the parent acid [*closo*-1-CB$_9$H$_9$-1-COOH]$^-$ (**9**), giving [*closo*-1-CB$_9$H$_9$-1-NH$_2$]$^-$ (**10-C1**).[23]

Transformations at the B(10) position began with the Pd(0)-catalyzed Buchwald–Hartwig amination of iodo acid **3**.[24] Using excess lithium hexamethyldisilazane (LiHMDS) as the ammonia equivalent and 2-(dicyclohexylphosphine)biphenyl as the phosphine ligand,[21] the ratio of amino acid **11** to parent acid **9**, a deiodination byproduct, was as high as 5:1 (Scheme 4).[21,24] Using the same conditions, the 6-iodo acid **6** was converted to 6-amino acid **12** (Scheme 5).[25] Experiments demonstrated that the amination is substantially more difficult for the {CB$_9$} cluster than for aromatic halides.

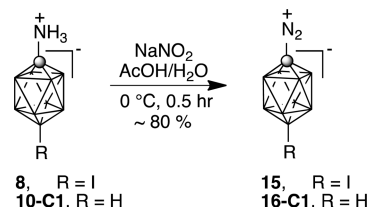The iodine in **3** was also replaced with an alkyl group via the standard Negishi coupling, providing, e.g., hexyl

SCHEME 5. 6-Amino Acids **12**
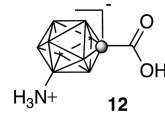
SCHEME 6. Alkylation of Iodo Acid **3** and Iodo Amine **8**
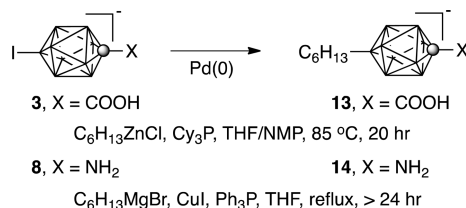
3, X = COOH	**13**, X = COOH
C$_6$H$_{13}$ZnCl, Cy$_3$P, THF/NMP, 85 °C, 20 hr	
8, X = NH$_2$	**14**, X = NH$_2$
C$_6$H$_{13}$MgBr, CuI, Ph$_3$P, THF, reflux, > 24 hr	

SCHEME 7. Preparation of Dinitrogen Derivative [*closo*-1-CB$_9$H$_8$-1-N$_2$-10-R] (**15** and **16-C1**)


| **8**, R = I | **15**, R = I |
| **10-C1**, R = H | **16-C1**, R = H |

derivative **13** (Scheme 6).[22] Similarly, alkylation of iodo amine **8** by typical Kumada coupling gave hexyl amine **14** as the sole product (Scheme 6).[26] In both reactions, a phosphonium zwitterion, resulting from replacement of iodine with the phosphine ligand, was observed as a byproduct.

N$_2^+$ Derivatives of the [*closo*-1-CB$_9$H$_{10}$]$^-$ Cluster. With access to both C(1) and B(10) amines, we focused on the preparation of apical dinitrogen derivatives and their reactions with nucleophiles. Diazotization of [*closo*-1-CB$_9$H$_8$-1-NH$_3$-10-R] (**8**, R = I; **10-C1**, R = H) was performed in aqueous AcOH, giving [*closo*-1-CB$_9$H$_8$-1-N$_2$-10-R] (**15**, R = I; **16-C1**, R = H) as a white precipitate (Scheme 7).[22,23]

Diazotization of amino acid **11** was surprisingly difficult, and reaction under the conditions used for the C(1) amines **8** and **10-C1** led to full recovery of unreacted **11**. Amino-*closo*-borates are known to be unusually basic, which prompted us to explore the diazotization under basic conditions. In fact, diazotization of **11** and preparation of stable dinitrogen acid [*closo*-1-CB$_9$H$_8$-1-COOH-10-N$_2$] (**17**) was achieved with excess [NO]$^+$[PF$_6$]$^-$ in MeCN containing pyridine (Scheme 8).[24]

The two types of dinitrogen derivatives, the C(1)–N$_2^+$ (such as **16-C1**) and B(10)–N$_2^+$ (such as **17**), have different thermal stabilities. While the C(1) derivatives decompose

SCHEME 8. Preparation of Dinitrogen Acid [*closo*-1-CB$_9$H$_8$-1-COOH-10-N$_2$] (**17**)
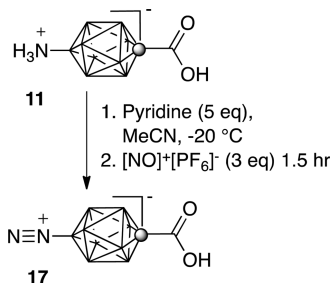
SCHEME 9. Thermolysis of [*closo*-1-CB$_9$H$_9$-1-N$_2$] (**16-C1**) in MeCN
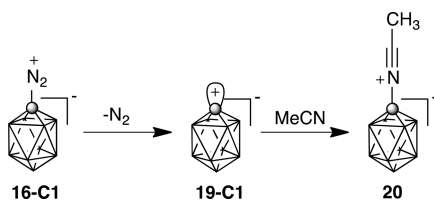
slowly in the solid state and more rapidly in solutions at ambient temperature, the B(10) derivatives are far more stable, and their thermal stability resembles that of dinitrogen derivatives of [*closo*-B$_{10}$H$_{10}$]$^{2-}$.[27] Temperature-dependent NMR kinetic measurements revealed a first order process with activation parameters $\Delta H^{\ddagger} = 38.4 \pm 0.8$ kcal mol^{-1} and $\Delta S^{\ddagger} = 44.5 \pm 2.5$ cal mol^{-1} K^{-1} in MeCN for [*closo*-1-CB$_9$H$_9$-1-N$_2$] (**16-C1**)[23] and $\Delta H^{\ddagger} = 33.9 \pm 1.4$ kcal mol^{-1} and $\Delta S^{\ddagger} = 10 \pm 3.5$ cal mol^{-1} K^{-1} for methyl ester [*closo*-1-CB$_9$H$_8$-1-COOMe-10-N$_2$] (**18**) in PhCN.[24] The rate-determining step in both reactions is the heterolytic cleavage of the N$_2^+$–boron cluster bond, leading to the formation of an electrophilic ylide: carbonium **19-C1** from dinitrogen **16-C1** (Scheme 9), and boronium from dinitrogen **18**. Subsequent reaction of the ylide with a nucleophilic solvent leads to a trapping product, such as **20**.

MP2-level computational analysis of the parent dinitrogen derivatives **16-C1** and [*closo*-1-CB$_9$H$_9$-10-N$_2$] (**16-B10**) demonstrated that the B(10) isomer is more thermodynamically stable by $\Delta H = 52.4$ kcal/mol and has a higher endotherm by 7.8 kcal mol^{-1} for the formation of the ylide relative to that of the C(1) isomer **16-C1**.[25] Consequently, the boronium ylide **19-B10** is more thermodynamically stable than the C(1) analogue **19-C1** by 44.6 kcal mol^{-1} and is less electrophilic, according to the energies of the LUMO (Figure 5).

The reactivity of [*closo*-1-CB$_9$H$_9$-1-N$_2$] (**16-C1**) was investigated with three types of nucleophiles: sulfur compounds, pyridine, and activated arenes. The reactions were conducted

19-C1, $E_{\text{LUMO}} = -1.57$ eV   **19-B10**, $E_{\text{LUMO}} = +0.21$ eV
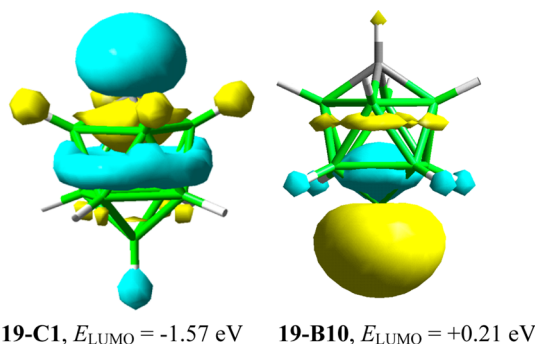
FIGURE 5. MP2/6-31G(d,p) derived contours and energies for the LUMO of ylides **19-C1** and **19-B10**.

SCHEME 10. Preparation of Sulfonium Derivative **24-C1** and Diazocoupling of **16-C1** with Phenolate and Aniline
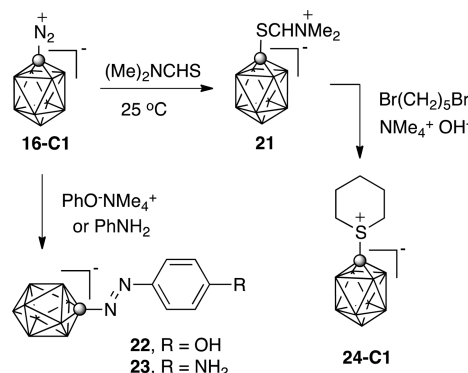
to understand the formation of sulfonium derivatives through a masked mercaptan, the formation of 1-pyridinium derivatives, and demonstration of a classical diazo coupling.[23]

Reaction of **16-C1** with *N,N*-dimethylthioformamide at ambient temperature gave zwitterion **21**, while reactions with phenolate anion and aniline provided azophenol **22** and azoaniline **23** as sole products (Scheme 10).[23] Alkylation of protected mercaptan **21** with 1,5-dibromopentane gave sulfonium derivative **24-C1** (Scheme 10).[23]

The reaction of **16-C1** with pyridine was most interesting. Thus, reaction in neat pyridine at ambient temperature gave a mixture of at least four products, instead of the anticipated **25a**.[23] The major component of the reaction mixture was identified as 2-isomer **25b**, while two minor more polar components were identified as **25c** and **25d** (Figure 6). At higher temperatures the composition of the mixture changed and the 1-isomer **25a** constituted 17% of the mixture. Interestingly, a reaction of **16-C1** with a 4% solution of pyridine in CH$_2$Cl$_2$ gave [*closo*-1-CB$_9$H$_9$-1-Cl]$^-$, while a reaction with a 4% solution of pyridine in benzene gave [*closo*-1-CB$_9$H$_9$-1-Ph]$^-$ as the major product. In both reactions, isomers **25a** and **25b** were formed in small quantities.
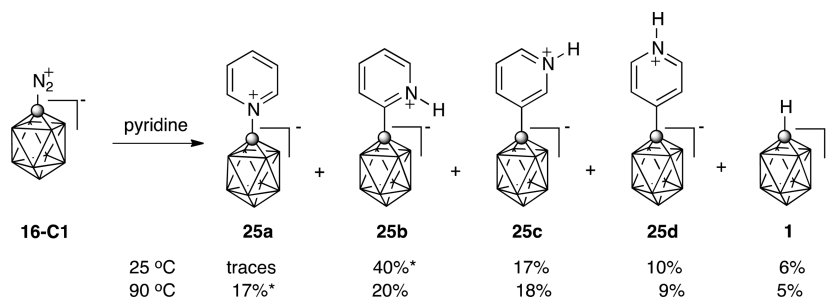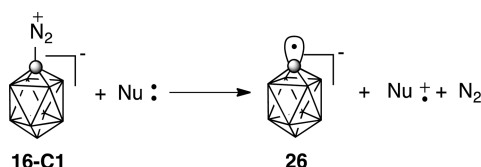
FIGURE 6. Product distributions in reaction of **16-C1** with neat pyridine. Asterisk denotes isolated yields.

SCHEME 11. Generation of Radical Anion **26**

The observed distribution of products suggests a radical pathway, which is consistent with the Gomberg–Bachmann radical arylation reaction. The process is initiated with single electron transfer (SET) from pyridine, a soft nucleophile, to **16-C1** (Scheme 11). After loss of N$_2$, the resulting radical anion **26** undergoes addition to the heteroaromatic ring, giving all four isomers **25**, among which **25b** dominates. For a mechanism involving the carbonium ylide **19-C1** as the intermediate, only one isomer, **25a**, is expected, as has been observed for dinitrogen derivatives of [closo-B$_{10}$H$_{10}$]$^{2-}$.[27,28] This rationale is consistent with a temperature-dependent distribution of products: at low temperature the SET mechanism operates nearly exclusively, yielding solely the C-isomers, while at high temperature the heterolysis of the C(1)–N$_2$ bond in **16-C1** is activated, giving rise to measurable quantities of the N-isomer **25a** (Figure 6).

Additional support for the radical mechanism was provided by electrochemical analysis of **16-C1**.[23] The reduction of **16-C1** is irreversible and more cathodic than that of PhN$_2^+$ by only 0.38 V, rendering **16-C1** similarly susceptible to SET from electron donors.

A similar mechanism involving radical ion **26** was postulated for the reaction of **16-C1** with other soft nucleophiles, such as Me$_2$S and Me$_2$NCHS, while with MeCN, a poor electron donor, only the heterolytic mechanism operates involving the ylide **19-C1**.

Using the transformations developed for the parent compound **16-C1**, several intermediates for liquid crystalline materials were prepared starting from iodo dinitrogen derivative **15**. This includes iodo derivatives **27** and **28**, which

upon Negishi coupling with alkylzinc gave the 10-alkyl derivatives **29** and **30[n]**, respectively (Scheme 12).[22,26,29]

Similar studies were conducted for acid [closo-1-CB$_9$H$_8$-1-COOH-10-N$_2$] (**17**), which was reacted with pyridine, sulfur compounds, and alcohol. Again, the reactions were conducted to prepare sulfonium and 1-pyridinium zwitterions at the B(10) position and to introduce a heteroatom link between the alkyl group and the B(10) position.[24] Thus, reactions of dinitrogen acid **17** in neat pyridine, 4-heptyloxypyridine, N,N-dimethylthioformamide, and pentanol gave pyridinium acids **31a** and **31b**, masked mercaptan **32**, and ionic pentyloxy acid **33**, respectively, as the sole products (Scheme 13).[24,30,31] With CH$_2$N$_2$, the dinitrogen acid **17** gave methyl ester **18**.[24]

The reaction of acid **17** with pyridine differs from that of the C(1) dinitrogen derivative **16-C1**. While the reaction of **16-C1** proceeded at ambient temperature and involved a radical anion, the reaction of dinitrogen acid **17** with pyridine required higher temperature and the formation of **31**, as the sole product, indicates domination by the heterolytic pathway involving a boronium ylide intermediate. Thus, the reactivity of **17** is similar to that of dinitrogen derivatives of the [closo-B$_{10}$H$_{10}$]$^{2-}$ cluster with pyridine, which also show enhanced thermal stability and reactivity implying involvement of a boronium ylide.[27] These characteristics of **17** are consistent with a significantly cathodic and reversible reduction potential of anion **17**$^-$ ($E_{1/2}$ = −1.21 V vrs SCE), which is apparently too low for effective SET from an electron donor to trigger the radical process.[24]

The synthetic utility of the protected mercaptan **32** was demonstrated by formation of sulfonium acids **34[n]** as shown in Scheme 14.[21,24,32]

Interestingly, the sulfonium acids **34[3]** and **34[5]** and their esters exist as equilibrium mixtures of configurational isomers *trans* and *cis* in a ratio of about 4:1 in solutions at ambient temperature, while only the *trans* isomer is observed for the series **28** and **30[n]**, in which the sulfonium fragment is substituted at the C(1) carbon. Temperature-dependent

SCHEME 12. Derivatives Prepared from [*closo*-1-CB₉H₈-1-N₂-10-I] (**15**)
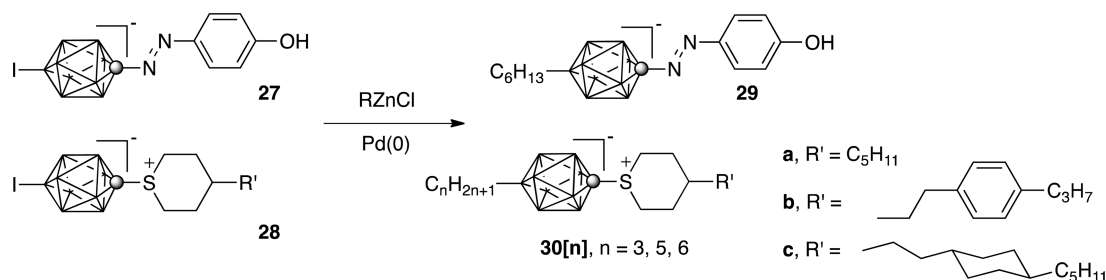
SCHEME 13. Transformations of Dinitrogen Acid **17**
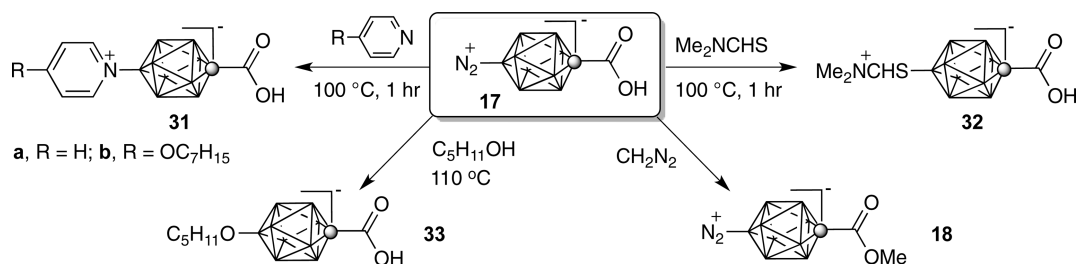
SCHEME 14. Preparation of Sulfonium Acid **34[n]**
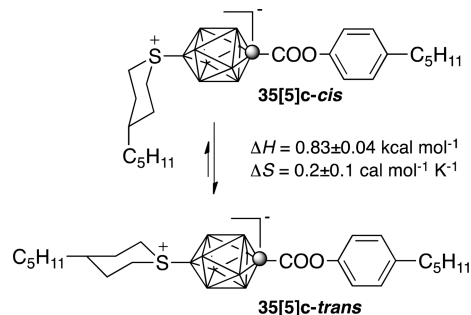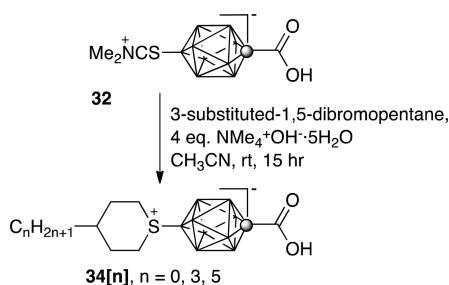

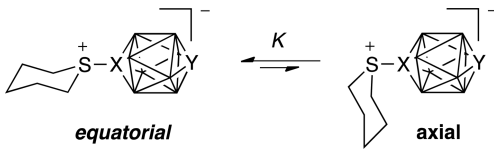**FIGURE 7.** Epimerization of Ester **35[5]c**

¹H NMR studies demonstrated that the equilibrium between the two isomers establishes quickly above ambient temperature, and yielded a difference in enthalpy, $\Delta H = 0.83 \pm 0.04$ kcal mol^{-1}, and entropy, $\Delta S = 0.2 \pm 0.1$ cal mol^{-1} K^{-1}, between **35[5]c-*cis*** and **35[5]c-*trans*** (Figure 7).[32]

Computational results for model compounds **24-C1** and **24-B10** are consistent with experimental observations.[32] The calculations demonstrated that **24-B10** has a low enthalpy of activation $\Delta H^{\ddagger} = 24.2$ kcal mol^{-1}, which is consistent with relatively fast isomerization observed for **35[5]c**, while $\Delta H^{\ddagger}$ for **24-C1** is higher by about 7 kcal/mol. Calculations also demonstrated that the low *cis/trans* equilibrium constant $K = 2$ for **24-B10** (experimental value for **35[5]c** is 3.8) at 298 K is due to a relatively long B(10)–S bond ($d_{S-B} = 1.854$ Å). In contrast, the C(1)–S bond in **24-C1** is shorter by nearly 0.1 Å, and consequently, the axial conformer is less favorable ($K = 42$). It is noteworthy that the molecular dipole moment is substantial (Table 1) and oriented along the long

molecular axis, rendering both **24-C1** and **24-B10** attractive structural elements for polar liquid crystals for display applications.

We also investigated the generation and reactivity of the dinitrogen acid [*closo*-1-CB₉H₈-1-COOH-6-N₂] (**36**) starting from 6-amino acid [*closo*-1-CB₉H₈-1-COOH-6-NH₃] (**12**).[25] Experiments using conditions for the analogous reaction of the 10-amino acid **11** indicated that the dinitrogen carboxylate anion **36**⁻ is unstable under the reaction conditions and decomposes to a 6-boronium ylide, which is trapped with the solvent. Diazotization of a mixture of amino acids **12** and **11** conducted in neat pyridine with [NO]⁺[BF₄]⁻ at −20 °C gave 6-pyridinium acid **37a** as the sole product, and trace amounts of dinitrogen acid **17** formed from **11** (Scheme 15).[25]

The reaction was extended to other heterocyclic bases. Diazotization of a mixture of amino acids **12** and **11** in

TABLE 1. Molecular Parameters for **24**[a]

compd	$\Delta H^{\ddagger}$/(kcal mol^{-1})	ΔG_{298}/(kcal mol^{-1})	K_{298}	d_{S-X}[b]/Å	μ[c]/D
24-C1, X = C, Y = BH	31.2	2.2	1/42	1.754	14.4
24-B10, X = B, Y = CH	24.2	0.4	1/2	1.856	8.75

[a]MP2/6-31G(d,p) level calculations with B3LYP/6-31G(d,p) thermodynamic corrections. [b]Distance between the S and the cage's C or B atoms in the axial conformer. [c]Dipole moment of the equatorial conformer.

SCHEME 15. Diazotization Reactions of Amino Acids **11** and **12** in Heterocyclic Bases
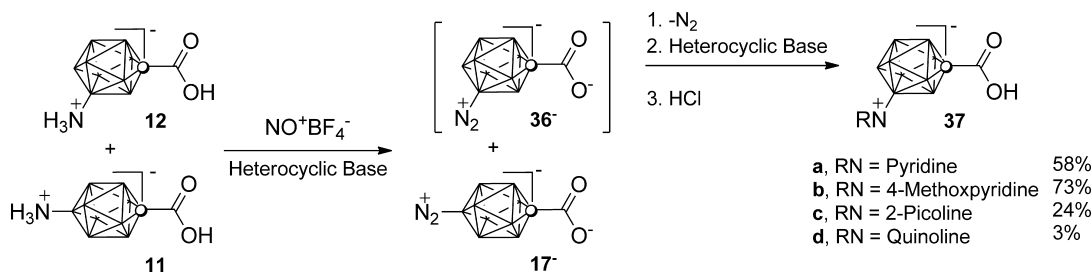
TABLE 2. Selected Thermodynamic Parameters for Isomeric Derivatives of **1**[a]

X	parameter	B10	B6	B2	C1
NH$_3^+$ **10**	pK_a	22.8	18.1	16.5	9.1
N$_2^+$ **16**	ΔG_{298} **16** to **19** kcal/mol	30.9	18.1	23.2	22.8
+ (ylide) **19**	E_{LUMO} /eV	0.21	0.40	-0.06	-1.57

[a]Reference **25**.

4-methoxypyridine gave 6-onium acid **37b** in high yield. In contrast, reactions in 2-picoline and quinoline gave incomplete conversion of **12** and low yields of the 6-onium products **37c** and **37d**, and no diazotization of the 10-amino acid **11** was observed. These results were attributed to the interference of the Me group in NO$^+$ transfer from 2-picoline and lower basicity of quinoline as compared to pyridine.

The lack of diazotization of 10-amino acid **11** in less basic quinoline and marginal reaction of 6-amino acid **12** are consistent with the calculated lower acidity of the protonated parent B(10)−amine **10-B10** than that of B(6)−amine

10-B6 (Table 2). The calculations for a set of isomeric dinitrogen derivatives **16** are also consistent with the observed significantly lower thermal stability of the 6-dinitrogen carboxylate **36**$^-$, relative to the 10-dinitrogen isomer **17**$^-$, and with the general order of stability of dinitrogen derivatives of **1**: B(10)−N$_2$ > C(1)−N$_2$ > B(6)−N$_2$. Thus, the MP2-level results predict a nearly 13 kcal/mol lower ΔG_{298} for dediazotization of **16-B6** and formation of 6-ylide **19-B6**, than for the 10-dinitrogen isomer **16-B10**. Interestingly, the thermal stability of the 2-dinitrogen derivative **16-B2** is predicted to be similar to that of the isolable stable
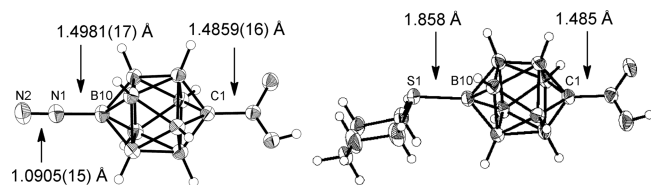
FIGURE 8. Thermal ellipsoid diagram of [*closo*-1-CB$_9$H$_8$-1-COOH-10-N$_2$] (**17**) and [*closo*-1-CB$_9$H$_8$-1-COOH-10-C$_5$H$_{10}$S] (**34[0]**) drawn at 50% probability. Adapted with permission from ref 24. Copyright 2010 American Chemical Society.

1-dinitrogen derivative **16-C1**. The reactivity of the resulting ylides **19** varies, and judging from the energy of the LUMO, the least electrophilic ylide is **19-B6**, while the most is **19-C1**.

Molecular Structures and Conformational Properties of the [*closo*-1-CB$_9$H$_{10}$]$^-$ Derivatives. Molecular structures of several derivatives, including dinitrogen derivatives **15**[33] and **17**,[24] pyridinium **25b**,[33] **31a**[24] and **37a**,[25] sulfonium acid **34[0]**,[24] azo aniline **23**,[33] and quinuclidinium **38**,[26] were established by single crystal XRD studies and compared to DFT computational results. Two examples of XRD analysis with indicated pertinent interatomic distances are shown in Figure 8.

Analysis of the {*closo*-1-CB$_9$} cage geometry for a number of structures indicates that the pyramidalization of the B(10) apex is greater for more electronegative onium substituents. The X−B(10) distance is smaller, and consequently, the B(10)···C(1) separation is markedly shorter in dinitrogen acid **17** ($d_{B(10)\ldots C(1)} = 3.429$ Å), with the most electronegative substituent N$_2^+$ than in the sulfonium **34[0]** ($d_{B(10)\ldots C(1)} = 3.478$ Å) and **31a** pyridinium ($d_{B(10)\ldots C(1)} = 3.471$ Å) analogs.[24]

Conformational properties and, hence, the rigidity and dynamic molecular shape impact mesogenic properties. Both experimental and theoretical analyses indicate that both the C(1)-carboxyl and B(10)-pyridine ring adopt a staggered orientation with respect to the {*closo*-1-CB$_9$} cage in the conformational minimum. As a consequence, the ideal dihedral angle between the planes of the two substituents is 45° and all conformers of acid **31** are chiral (Figure 9). DFT results demonstrated that the thian ring at the B(10) and C(1) positions prefers staggered conformations relative to the cage in which the sulfur lone pair eclipses the B−B or C−B bond. Consequently, the acid **34[0]** has a C$_s$-symmetric conformational minimum, although in the crystal structure the sulfonium ring is twisted by up to 30° away from the ideal staggered position. DFT analysis of the B(10) alkyl and alkoxy derivatives **13** and **33** demonstrated that the substituents are staggered and eclipsed relative to the cage, respectively, resulting in chiral conformers in the former and a C$_s$-symmetric molecule for acid **33**.
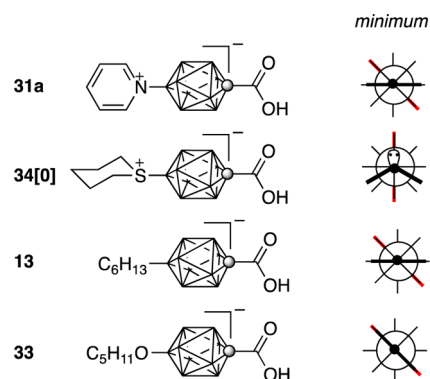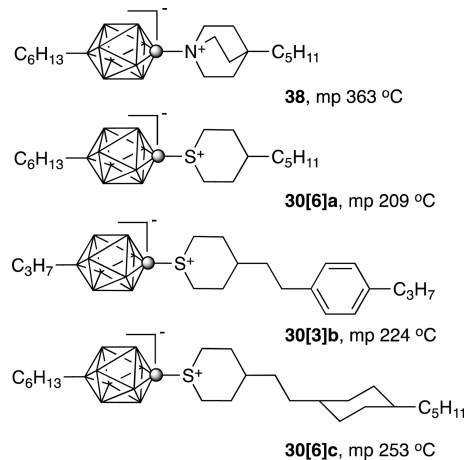

FIGURE 9. Extended Newman projection along the long molecular axes of conformational minima for selected acids. The bars represent the substituents, and the filled circle is the connecting heteroatom or CH$_2$ in **13**.

CHART I. Examples of Polar Materials **30[n]** and **38** (Type **V**)

Liquid Crystals Derived from the [*closo*-1-CB$_9$H$_{10}$]$^-$ Cluster. The developed chemistry of the [*closo*-1-CB$_9$H$_{10}$]$^-$ anion (**1**) permitted the preparation of the first examples of two new classes of materials: polar zwitterionic (**V** and **VI**) and anion-driven ionic liquid crystals (**VII**). The polar materials **V** studied thus far, C(1)-sulfonium **30[n]** and C(1)-quinuclidinium **38**, do not form liquid crystalline phases (Chart I).[26,29] They exhibit high melting points and limited solubility in other liquid crystalline materials; nevertheless, they significantly increase the dielectric anisotropy, $\Delta\varepsilon$, of the host.[26] For example, compound **38**, with the calculated longitudinal dipole moment component $\mu_{\parallel} = 15.9$ D, exhibits a large value of $\Delta\varepsilon = 70 \pm 1$ extrapolated to infinite dilution in a nematic host, and a relatively high virtual clearing temperature, $[T_{NI}] = 139 \pm 1$.[26]

Polar materials **VI**, such as pyridinium esters **39** and sulfonium esters **35[n]**, were more promising than materials **V** (Chart II). Esters **39** have lower melting points, have greater

CHART II. Examples of Polar Materials (Type **VI**)

39

35[n], n = 3, 5

a: R = C_5H_{11} **b:** R = C_5H_{11}

R =   X   **c:** X = C_5H_{11}; **d:** X = OC$_4$H$_9$;
             e: X = CN; **f:** X = OCF$_3$

g: R =   **h:** R = C_6H_{13}

$C_7H_{15}O$ N$^+$-B   COO C_5H_{11}
39c   Cr 121 (N 114) I, $\Delta\varepsilon$ = 42

$C_7H_{15}O$ C–C   COO C_5H_{11}
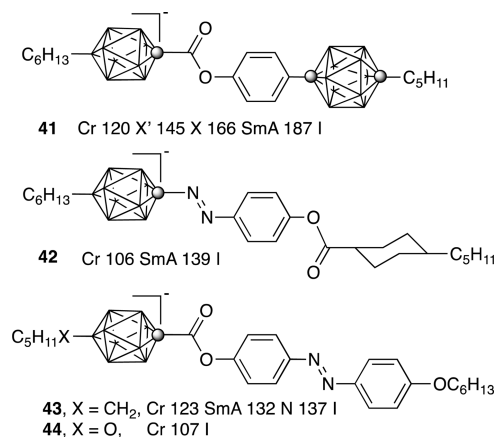**40c**   Cr 45 N 105 I
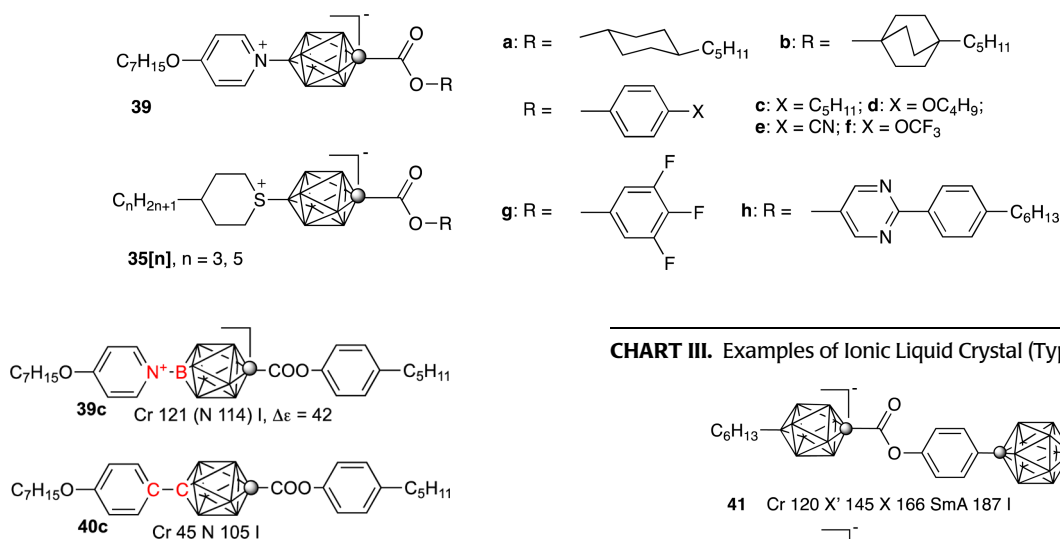
FIGURE 10. Polar and nonpolar isosteric derivatives **39c** and **40c**.

compatibility with liquid crystalline hosts, and form nematic phases above 100 °C. Analysis of their dielectric properties in dilute nematic solutions revealed extrapolated dielectric anisotropy, $\Delta\varepsilon$, typically around 40, but a record high value of $\Delta\varepsilon$ = 113 was measured for cyanophenol ester **39e**.[31,32]

Esters **39** permitted for the first time the effect of a dipole moment on the stability of the nematic phase to be examined experimentally.[31] This was accomplished by comparing polar and nonpolar isosteric pairs of the [*closo*-1-CB$_9$H$_{10}$]$^-$ anion and isoelectronic *p*-carborane, [*closo*-1,10-C$_2$B$_8$H$_{10}$]. Replacement of a polar B$^-$–N$^+$ fragment in **39** with a nonpolar C–C fragment provided compounds **40** with drastically different dipole moments (calculated $\Delta\mu \approx$ 12 D for all pairs), but with essentially identical geometrical and conformational properties (Figure 10).

The results for pairs of compounds such as **39c** and **40c** (Figure 10) demonstrated that a longitudinal dipole moment's effect on phase properties strongly depends on the nature of the substituent distant from the zwitterion center.[31] Thus, esters of cycloalkanols **39a/40a** and **39b/40b** with the increased longitudinal dipole have higher phase stability by about 55 K. A much smaller increase in T_{NI} of only 9 K is observed for the analogous pentylphenol esters **39c/40c**, and even moderate nematic phase destabilization is found for the cyanophenol esters **39e/40e**, despite the same difference in the molecular dipole moment. These results suggest close intermolecular contact and dielectric screening of the dipoles.

Esters **35[n]** derived from sulfonium acids represent examples of a new class of shape-shifting nematic material,

CHART III. Examples of Ionic Liquid Crystal (Type **VII**)^a

41   Cr 120 X' 145 X 166 SmA 187 I

42   Cr 106 SmA 139 I

43, X = CH$_2$, Cr 123 SmA 132 N 137 I
44, X = O,   Cr 107 I

^{a}Each anion is accompanied by 1-butyl-4-heptyloxypyridinium.

where the molecule can exist in two different shapes (linear or bent) due to facile isomerization at the sulfur center.[29,32] This results in improved solubility in the nematic hosts and lower transition temperatures T_{NI}, when compared to esters of pyridinium acid **31b**.

Ion pairs with anisometric anions derived from hexyl acid **13** or phenol **29** exhibit liquid crystalline phases and represent the first examples of anion-driven ILCs (type **VII**). Typically, these materials possess the characteristic smectic A phase (**41**–**43**, Chart III), commonly exhibited by ILC, and occasionally a soft crystalline phase (**41**).[22,34] Surprisingly, compound **43** exhibits a nematic phase, which is rarely observed in ILCs.[34] Binary mixture studies demonstrated that ILCs **VII** are miscible with nonionic LCs, which is promising for formulation of materials for metal ion conduction.

Interestingly, replacement of the connecting X = CH$_2$ group in ionic liquid crystal **43** with an oxygen atom in **44** resulted in significant destabilization of the nematic and, to a greater extent, SmA phases, as established from binary mixture studies in the {*closo*-1-CB$_{11}$} analogue of **43**.[35] DFT modeling of both anions suggests that the destabilization results from the

difference in charge distribution rather than conformational changes.

Further examples of polar and ionic liquid crystals derived from the [*closo*-1-CB$_9$H$_{10}$]$^-$ anion are being investigated in our laboratory with the focus on greater compatibility with nematic materials and ion pairs with the Li$^+$ cation.

Summary

This Account presented a snapshot of the rapid development of the fundamental chemistry of the [*closo*-1-CB$_9$H$_{10}$]$^-$ anion (**1**). Three key advancements in the fundamental chemistry of **1** were highlighted: (*i*) the multigram scale preparation of the isomerically pure 1,10-disubstituted derivative, iodo acid **3**, (*ii*) functional group transformations at the C(1) position, and (*iii*) functional group transformations at the B(10) position. Transformations of iodo acid **3** have led to other important intermediates, such as dinitrogen derivatives **15** and **17**. These developments have opened up exciting possibilities for application of anion **1** as a structural element in a variety of molecular and polymeric materials, including the new classes of polar (**V** and **VI**) and ionic liquid crystals (**VII**).

BIOGRAPHICAL INFORMATION

Bryan Ringstrand received his Ph.D. degree in 2011 at Vanderbilt University, where he worked with Prof. Piotr Kaszynski. He is currently a postdoctoral appointee at Argonne National Laboratory.

Piotr Kaszynski received his M.S. degree from Warsaw Polytechnic (1985) and subsequently his Ph.D. from University of Texas (1991). After a postdoctoral appointment at Caltech, he joined the faculty of Vanderbilt University (1993) and University of Łódź (2010). His research interests are in the areas of molecular materials, liquid crystals, boron clusters, stable radicals, and strained polycyclic systems.

FOOTNOTES

REFERENCES

1 Williams, R. E. The polyborane, carborane, carbocation continuum: architectural patterns. *Chem. Rev.* **1992**, *92*, 177–207.

2 Todd, L. J. The Chemistry of Polyhedral Borane Ions. In *Progress in Boron Chemistry*; Brotherton, R. J., Steinberg, H., Eds.; Pergamon Press: New York, 1970; Vol. 2; pp 1−35.

3 *Boron Science. New Technologies and Applications*; Hosmane, N. S., Ed.; CRC Press: New York, 2012.

4 Grimes, R. N. *Carboranes*, 2nd ed; Academic Press: 2011.

5 Reed, C. A. Carboranes: A New Class of Weakly Coordinating Anions for Strong Electrophiles, Oxidants, and Superacids. *Acc. Chem. Res.* **1998**, *31*, 133–139.

6 Körbe, S.; Schreiber, P. J.; Michl, J. Chemistry of the Carba-closo-dodecaborate(−) Anion, CB$_{11}$H$_{12}$$^-$. *Chem. Rev.* **2006**, *106*, 5208–5249.

7 Knoth, W. H. B$_{10}$H$_{12}$CNH$_3$, B$_9$H$_9$CH$^-$, B$_{11}$H$_{11}$CH$^-$, and metallomonocarboranes. *Inorg. Chem.* **1971**, *10*, 598–605.

8 Nestor, K.; Štibr, B.; Kennedy, J. D.; Thornton-Pett, M.; Jelínek, T. Ten-Vertex Monocarborane Chemistry. A Convenient New Preparation of the [closo-1-CB$_9$H$_{10}$]$^-$ Anion and the Crystal and Molecular Structure of [(η5-C$_5$Me$_5$)Ir$_2$Cl$_3$]$^+$ [closo-1-CB$_9$H$_{10}$]$^-$. *Collect. Czech. Chem. Commun.* **1992**, *57*, 1262–1268.

9 Jelínek, T.; Štibr, B.; Plešek, J.; Thornton-Pett, M.; Kennedy, J. D. Ten-vertex monocarborane chemistry. Synthesis of carbon-substituted ligand derivatives 1-L-closo-1-CB$_9$H$_9$ and crystal and molecular structure of 1-(Me$_3$N)-closo-1-CB$_9$H$_9$. *J. Chem. Soc., Dalton Trans.* **1997**, 4231–4236.

10 Tsnag, C.-W.; Yang, Q.; Sze, T.-P. E.; Mak, T. C. W.; Chan, D. T. W.; Xie, Z. Synthesis and Structural Characterization of Highly Chlorinated, Brominated, Iodinated, and Methylated Carborane Anions, 1-H-CB$_9$X$_9$$^-$, 1-NH$_2$-CB$_9X_9$$^-$ (X = Cl, Br, I), and 1-H-CB$_9$(CH^3)$_9$$^-$. *Inorg. Chem.* **2000**, *39*, 3582–3589.

11 Ivanov, S. V.; Rockwell, J. J.; Miller, S. M.; Anderson, O. P.; Solntsev, K. A.; Strauss, S. H. Reactions of CB$_9$H$_{10}$$^-$ with Electrophiles, Including the Regioselective Mono- and Dihalogenation of the Lower Belt. *Inorg. Chem.* **1996**, *35*, 7882–7891.

12 Franken, A.; Kilner, C. A.; Thornton-Pett, M.; Kennedy, J. D. Polyhedral Monocarborane Chemistry. A Review of Recent Developments Among C-Aryl Monocarborane Systems. *Collect. Czech. Chem. Commun.* **2002**, *67*, 869–912.

13 Brellochs, B.; Bačkovský, J.; Štibr, B.; Jelínek, T.; Holub, J.; Bakardjiev, M.; Hnyk, D.; Hofmann, M.; Císarová, I.; Wrackmeyer, B. New Ways to a Series of Parent Representatives of the Eight-, Nine-, and Ten-Vertex Monocarborane Family. *Eur. J. Inorg. Chem.* **2004**, 3605–3611.

14 Sivaev, I. B.; Starikova, Z. A.; Petrovskii, P. V.; Bregadze, V. I.; Sjöberg, S. The synthesis of functional derivatives of the [1-CB$_9$H$_{10}$]$^-$ anion by Brellochs reaction. *J. Organomet. Chem.* **2005**, *690*, 2790–2795.

15 Franken, A.; Carr, M. J.; Clegg, W.; Kilner, C. A.; Kennedy, J. D. Monocarborane anion chemistry. {COOH}, {CH$_2$OH} and {CHO} units as functional groups on ten-vertex monocarborane anionic compounds. *Dalton Trans.* **2004**, 3552–3561.

16 Franken, A.; Bullen, N. J.; Jelínek, T.; Thornton-Pett, M.; Teat, S. J.; Clegg, W.; Kennedy, J. D.; Hardie, M. J. Structural chemistry of halogenated monocarbaboranes: the extended structures of Cs[1-HCB$_9$H$_4$Br$_5$], Cs[1-HCB$_{11}$H$_5$Cl$_6$] and Cs[1-HCB$_{11}$H$_5$Br$_6$]. *New J. Chem.* **2004**, *28*, 1499–1505.

17 Schwab, P. F. H.; Levin, M. D.; Michl, J. Molecular Rods. 1. Simple Axial Rods. *Chem. Rev.* **1999**, *99*, 1863–1933.

18 Kaszynski, P. closo-Boranes as Structural Elements for Liquid Crystals. In *Boron Science. New Technologies and Applications*; Hosmane, N. S., Ed.; CRC Press: New York, 2012; pp 319−354.

19 Demus, D. Chemical Structure and Mesogenic Properties. In *Handbook of Liquid Crystals*; Goodby, J. W., Gray, G. W., Spiess, H.-W., Vill, V., Eds.; Wiley-VCH: New York, 1998; Vol. 1; pp 133−187.

20 Ringstrand, B.; Balinski, A.; Franken, A.; Kaszynski, P. A Practical Synthesis of Isomerically Pure 1,10-Difunctionalized Derivatives of the [closo-1-CB$_9$H$_{10}$] Anion. *Inorg. Chem.* **2005**, *44*, 9561–9566.

21 Pecyna, J.; Denicola, R. P.; Ringstrand, B.; Jankowiak, A.; Kaszynski, P. The preparation of [closo-1-CB$_9$H$_8$-1-COOH-10-(4-C$_3$H$_7$C$_5$H$_9$S)] as intermediate to polar liquid crystals. *Polyhedron* **2011**, *30*, 2505–2513.

22 Ringstrand, B.; Monobe, H.; Kaszynski, P. Anion-driven mesogenicity: ionic liquid crystals based on the [closo-1-CB$_9$H$_{10}$]$^-$ cluster. *J. Mater. Chem.* **2009**, *19*, 4805–4812.

23 Ringstrand, B.; Kaszynski, P.; Franken, A. Synthesis and Reactivity of [closo-1-CB$_9$H$_9$-1-N$_2$]: Functional Group Interconversion at the Carbon Vertex of the {closo-1-CB$_9$} Cluster. *Inorg. Chem.* **2009**, *48*, 7313–7329.

24 Ringstrand, B.; Kaszynski, P.; Young, V. G., Jr.; Janoušek, Z. Anionic Amino Acid [closo-1-CB$_9$H$_8$-1-COO-10-NH$_3$]$^-$ and Dinitrogen Acid [closo-1-CB$_9$H$_8$-1-COOH-10-N$_2$] as Key Precursors to Advanced Materials: Synthesis and Reactivity. *Inorg. Chem.* **2010**, *49*, 1166–1179.

25 Ringstrand, B.; Kaszynski, P.; Young, V. G., Jr. Diazotization of the Amino Acid [closo-1-CB$_9$H$_8$-1-COOH-6-NH$_3$] and Reactivity of the [closo-1-CB$_9$H$_8$-1-COO-6-N$_2$]$^-$ Anion. *Inorg. Chem.* **2011**, *50*, 2654–2660.

26 Ringstrand, B.; Kaszynski, P.; Januszko, A.; Young, V. G., Jr. Polar derivatives of the [closo-1-CB$_9$H$_{10}$]$^-$ cluster as positive $\Delta\varepsilon$ additives to nematic hosts. *J. Mater. Chem.* **2009**, *19*, 9204–9212.

27 Knoth, W. H. Chemistry of Boranes. XXVI.1 Inner Diazonium Salts 1,10-B$_{10}$H$_8$(N$_2$)$_2$, -B$_{10}$Cl$_8$(N$_2$)$_2$, and -B$_{10}$I$_8$(N$_2$)$_2$. *J. Am. Chem. Soc.* **1966**, *88*, 935–939.

28 Kaszynski, P.; Huang, J.; Jenkins, G. S.; Bairamov, K. A.; Lipiak, D. Boron Clusters in Liquid Crystals. *Mol. Cryst. Liq. Cryst.* **1995**, *260*, 315–332.

29 Pecyna, J.; Ringstrand, B.; Kaszynski, P.; Bremer, M. Unpublished results.

30 Pecyna, J.; Ringstrand, B.; Kaszynski, P. Transmission of electronic effects through the {closo-1-CB$_9$} and {closo-1-CB$_{11}$} cages: Dissociation constants for a series of [closo-1-CB$_9$H$_8$-1-COOH-10-X] and [closo-1-CB$_{11}$H$_{10}$-1-COOH-12-X] acids. *Inorg. Chem.* **2012**, *51*, 5353–5359.

31 Ringstrand, B.; Kaszynski, P. How much can an electric dipole stabilize a nematic phase? Polar and non-polar isosteric derivatives of [closo-1-CB$_9$H$_{10}$]$^-$ and [closo-1,10-C$_2$B$_8$H$_{10}$]. *J. Mater. Chem.* **2010**, *20*, 9613–9615.

32 Ringstrand, B.; Kaszynski, P. High $\Delta\varepsilon$ nematic liquid crystals: fluxional zwitterions of the [closo-1-CB$_9$H$_{10}$]$^-$ cluster. *J. Mater. Chem.* **2011**, *21*, 90–95.

33 Carr, M. J.; Kaszynski, P.; Franken, A.; Kennedy, J. D. Unpublished results.

34 Ringstrand, B.; Jankowiak, A.; Johnson, L. E.; Kaszynski, P.; Pociecha, D.; Górecka, E. Anion-driven mesogenicity: a comparative study of ionic liquid crystals based on the [closo-1-CB$_9$H$_{10}$]$^-$ and [closo-1-CB$_{11}$H$_{12}$]$^-$ clusters. *J. Mater. Chem.* **2012**, *22*, 4874–4880.

35 Pecyna, J.; Sivaramamoorthy, A.; Jankowiak, A.; Kaszynski, P. Anion driven ionic liquid crystals: The effect of the connecting group in [closo-1-CB$_9$H$_{10}$]$^-$ derivatives on mesogenic properties. *Liq. Cryst.* **2012**, *39*, 965–971.